

PDF hosted at the Radboud Repository of the Radboud University Nijmegen

The following full text is a preprint version which may differ from the publisher's version.

For additional information about this publication click this link.

<http://hdl.handle.net/2066/124603>

Please be advised that this information was generated on 2021-09-22 and may be subject to change.

Search for Excited Leptons in e^+e^- Collisions at $\sqrt{s} = 130$ and 136 GeV

The OPAL Collaboration

Abstract

We have searched for excited states of charged and neutral leptons, e^* , μ^* , τ^* and ν^* , in e^+e^- collisions at $\sqrt{s} = 130$ and 136 GeV using the OPAL detector at LEP. No evidence for their existence was found. With the most common coupling assumptions, the final states from excited lepton pair production include $\ell^+\ell^-\gamma\gamma$ and $\ell^+\ell^-WW$ (with the subsequent decay of the virtual W bosons). From the analysis of these final states, 95% confidence level lower mass limits of 66.5 GeV for e^* , 66.8 GeV for μ^* , 65.3 GeV for τ^* , 66.2 GeV for ν_e^* , 66.5 GeV for ν_μ^* and 64.7 GeV for ν_τ^* are inferred. From the analysis of $\gamma\gamma$ final states with missing energy and using alternative coupling assignments which permit photonic ν^* decays, a 95% confidence level lower mass limit of 65.0 GeV for each ν^* flavour is inferred. From the analysis of the $\ell^+\ell^-\gamma$, acoplanar lepton pair, and single γ final states expected from excited lepton single production, upper limits on f/Λ (ratio of the coupling to the compositeness scale) are determined for excited lepton masses up to the kinematic limit.

Submitted to Physics Letters B

The OPAL Collaboration

G. Alexander²³, J. Allison¹⁶, N. Altekamp⁵, K. Ametewee²⁵, K.J. Anderson⁹, S. Anderson¹², S. Arcelli², S. Asai²⁴, D. Axen²⁹, G. Azuelos^{18,a}, A.H. Ball¹⁷, E. Barberio⁸, R.J. Barlow¹⁶, R. Bartoldus³, J.R. Batley⁵, J. Bechtluft¹⁴, C. Beeston¹⁶, T. Behnke⁸, A.N. Bell¹, K.W. Bell²⁰, G. Bella²³, S. Bentvelsen⁸, P. Berlich¹⁰, S. Bethke¹⁴, O. Biebel¹⁴, V. Blobel⁸, I.J. Bloodworth¹, J.E. Bloomer¹, M. Bobinski¹⁰, P. Bock¹¹, H.M. Bosch¹¹, M. Boutemur³⁴, B.T. Bouwens¹², S. Braibant¹², R.M. Brown²⁰, H.J. Burckhart⁸, C. Burgard⁸, R. Bürgin¹⁰, P. Capiluppi², R.K. Carnegie⁶, A.A. Carter¹³, J.R. Carter⁵, C.Y. Chang¹⁷, C. Charlesworth⁶, D.G. Charlton^{1,b}, D. Chrisman⁴, S.L. Chu⁴, P.E.L. Clarke¹⁵, I. Cohen²³, J.E. Conboy¹⁵, O.C. Cooke¹⁶, M. Cuffiani², S. Dado²², C. Dallapiccola¹⁷, G.M. Dallavalle², S. De Jong¹², L.A. del Pozo⁸, K. Desch³, M.S. Dixit⁷, E. do Couto e Silva¹², M. Doucet¹⁸, E. Duchovni²⁶, G. Duckeck³⁴, I.P. Duerdoth¹⁶, J.E.G. Edwards¹⁶, P.G. Estabrooks⁶, H.G. Evans⁹, M. Evans¹³, F. Fabbri², P. Fath¹¹, F. Fiedler¹², M. Fierro², H.M. Fischer³, R. Folman²⁶, D.G. Fong¹⁷, M. Foucher¹⁷, A. Fürtjes⁸, P. Gagnon⁷, A. Gaidot²¹, J.W. Gary⁴, J. Gascon¹⁸, S.M. Gascon-Shotkin¹⁷, N.I. Geddes²⁰, C. Geich-Gimbel³, F.X. Gentit²¹, T. Geralis²⁰, G. Giacomelli², P. Giacomelli⁴, R. Giacomelli², V. Gibson⁵, W.R. Gibson¹³, D.M. Gingrich^{30,a}, D. Glenzinski⁹, J. Goldberg²², M.J. Goodrick⁵, W. Gorn⁴, C. Grandi², E. Gross²⁶, M. Gruwé⁸, C. Hajdu³², G.G. Hanson¹², M. Hansroul⁸, M. Hapke¹³, C.K. Hargrove⁷, P.A. Hart⁹, C. Hartmann³, M. Hauschild⁸, C.M. Hawkes⁵, R. Hawkings⁸, R.J. Hemingway⁶, G. Herten¹⁰, R.D. Heuer⁸, M.D. Hildreth⁸, J.C. Hill⁵, S.J. Hillier¹, T. Hilse¹⁰, P.R. Hobson²⁵, R.J. Homer¹, A.K. Honma^{28,a}, D. Horváth^{32,c}, R. Howard²⁹, R.E. Hughes-Jones¹⁶, D.E. Hutchcroft⁵, P. Igo-Kemenes¹¹, D.C. Imrie²⁵, M.R. Ingram¹⁶, K. Ishii²⁴, A. Jawahery¹⁷, P.W. Jeffreys²⁰, H. Jeremie¹⁸, M. Jimack¹, A. Joly¹⁸, C.R. Jones⁵, G. Jones¹⁶, M. Jones⁶, R.W.L. Jones⁸, U. Jost¹¹, P. Jovanovic¹, T.R. Junk⁸, D. Karlen⁶, K. Kawagoe²⁴, T. Kawamoto²⁴, R.K. Keeler²⁸, R.G. Kellogg¹⁷, B.W. Kennedy²⁰, B.J. King⁸, J. Kirk²⁹, S. Kluth⁸, T. Kobayashi²⁴, M. Kobel¹⁰, D.S. Koetke⁶, T.P. Kokott³, S. Komamiya²⁴, R. Kowalewski⁸, T. Kress¹¹, P. Krieger⁶, J. von Krogh¹¹, P. Kyberd¹³, G.D. Lafferty¹⁶, H. Lafoux²¹, R. Lahmann¹⁷, W.P. Lai¹⁹, D. Lanske¹⁴, J. Lauber¹⁵, S.R. Lautenschlager³¹, J.G. Layter⁴, D. Lazic²², A.M. Lee³¹, E. Lefebvre¹⁸, D. Lellouch²⁶, J. Letts², L. Levinson²⁶, C. Lewis¹⁵, S.L. Lloyd¹³, F.K. Loebinger¹⁶, G.D. Long¹⁷, M.J. Losty⁷, J. Ludwig¹⁰, A. Luig¹⁰, A. Malik²¹, M. Mannelli⁸, S. Marcellini², C. Markus³, A.J. Martin¹³, J.P. Martin¹⁸, G. Martinez¹⁷, T. Mashimo²⁴, W. Matthews²⁵, P. Mättig³, W.J. McDonald³⁰, J. McKenna²⁹, E.A. Mckigney¹⁵, T.J. McMahon¹, A.I. McNab¹³, R.A. McPherson⁸, F. Meijers⁸, S. Menke³, F.S. Merritt⁹, H. Mes⁷, J. Meyer²⁷, A. Michelini², G. Mikenberg²⁶, D.J. Miller¹⁵, R. Mir²⁶, W. Mohr¹⁰, A. Montanari², T. Mori²⁴, M. Morii²⁴, U. Müller³, K. Nagai²⁶, I. Nakamura²⁴, H.A. Neal⁸, B. Nellen³, B. Nijhar¹⁶, R. Nisius⁸, S.W. O’Neale¹, F.G. Oakham⁷, F. Odorici², H.O. Ogren¹², T. Omori²⁴, M.J. Oreglia⁹, S. Orito²⁴, J. Pálinkás^{33,d}, G. Pásztor³², J.R. Pater¹⁶, G.N. Patrick²⁰, J. Patt¹⁰, M.J. Pearce¹, S. Petzold²⁷, P. Pfeifenschneider¹⁴, J.E. Pilcher⁹, J. Pinfold³⁰, D.E. Plane⁸, P. Poffenberger²⁸, B. Poli², A. Posthaus³, H. Przysieznik³⁰, D.L. Rees¹, D. Rigby¹, S.A. Robins¹³, N. Rodning³⁰, J.M. Roney²⁸, A. Rooke¹⁵, E. Ros⁸, A.M. Rossi², M. Rosvick²⁸, P. Routenburg³⁰, Y. Rozen²², K. Runge¹⁰, O. Runolfsson⁸, U. Ruppel¹⁴, D.R. Rust¹², R. Rylko²⁵, K. Sachs¹⁰, E.K.G. Sarkisyan²³, M. Sasaki²⁴, C. Sbarra², A.D. Schaile³⁴, O. Schaile³⁴, F. Scharf³, P. Scharff-Hansen⁸, P. Schenk⁴, B. Schmitt⁸, S. Schmitt¹¹, M. Schröder⁸, H.C. Schultz-Coulon¹⁰, M. Schulz⁸, M. Schumacher³, P. Schütz³, W.G. Scott²⁰, T.G. Shears¹⁶, B.C. Shen⁴, C.H. Shepherd-Themistocleous²⁷, P. Sherwood¹⁵, G.P. Siroli², A. Sittler²⁷, A. Skillman¹⁵, A. Skuja¹⁷, A.M. Smith⁸, T.J. Smith²⁸,

G.A. Snow¹⁷, R. Sobie²⁸, S. Söldner-Rembold¹⁰, R.W. Springer³⁰, M. Sproston²⁰, A. Stahl³,
M. Starks¹², M. Steiert¹¹, K. Stephens¹⁶, J. Steuerer²⁷, B. Stockhausen³, D. Strom¹⁹,
F. Strumia⁸, P. Szymanski²⁰, R. Tafirout¹⁸, S.D. Talbot¹, S. Tanaka²⁴, P. Taras¹⁸, S. Tarem²²,
M. Tecchio⁸, M. Thiergen¹⁰, M.A. Thomson⁸, E. von Törne³, S. Towers⁶, T. Tsukamoto²⁴,
E. Tsur²³, A.S. Turcot⁹, M.F. Turner-Watson⁸, P. Utzat¹¹, R. Van Kooten¹², G. Vasseur²¹,
M. Verzocchi¹⁰, P. Vikas¹⁸, M. Vincter²⁸, E.H. Vokurka¹⁶, F. Wäckerle¹⁰, A. Wagner²⁷,
C.P. Ward⁵, D.R. Ward⁵, J.J. Ward¹⁵, P.M. Watkins¹, A.T. Watson¹, N.K. Watson⁷, P. Weber⁶,
P.S. Wells⁸, N. Wermes³, J.S. White²⁸, B. Wilkens¹⁰, G.W. Wilson²⁷, J.A. Wilson¹, G. Wolf²⁶,
S. Wotton⁵, T.R. Wyatt¹⁶, S. Yamashita²⁴, G. Yekutieli²⁶, V. Zacek¹⁸,

¹School of Physics and Space Research, University of Birmingham, Birmingham B15 2TT, UK

²Dipartimento di Fisica dell' Università di Bologna and INFN, I-40126 Bologna, Italy

³Physikalisches Institut, Universität Bonn, D-53115 Bonn, Germany

⁴Department of Physics, University of California, Riverside CA 92521, USA

⁵Cavendish Laboratory, Cambridge CB3 0HE, UK

⁶ Ottawa-Carleton Institute for Physics, Department of Physics, Carleton University, Ottawa, Ontario K1S 5B6, Canada

⁷Centre for Research in Particle Physics, Carleton University, Ottawa, Ontario K1S 5B6, Canada

⁸CERN, European Organisation for Particle Physics, CH-1211 Geneva 23, Switzerland

⁹Enrico Fermi Institute and Department of Physics, University of Chicago, Chicago IL 60637, USA

¹⁰Fakultät für Physik, Albert Ludwigs Universität, D-79104 Freiburg, Germany

¹¹Physikalisches Institut, Universität Heidelberg, D-69120 Heidelberg, Germany

¹²Indiana University, Department of Physics, Swain Hall West 117, Bloomington IN 47405, USA

¹³Queen Mary and Westfield College, University of London, London E1 4NS, UK

¹⁴Technische Hochschule Aachen, III Physikalisches Institut, Sommerfeldstrasse 26-28, D-52056 Aachen, Germany

¹⁵University College London, London WC1E 6BT, UK

¹⁶Department of Physics, Schuster Laboratory, The University, Manchester M13 9PL, UK

¹⁷Department of Physics, University of Maryland, College Park, MD 20742, USA

¹⁸Laboratoire de Physique Nucléaire, Université de Montréal, Montréal, Quebec H3C 3J7, Canada

¹⁹University of Oregon, Department of Physics, Eugene OR 97403, USA

²⁰Rutherford Appleton Laboratory, Chilton, Didcot, Oxfordshire OX11 0QX, UK

²¹CEA, DAPNIA/SPP, CE-Saclay, F-91191 Gif-sur-Yvette, France

²²Department of Physics, Technion-Israel Institute of Technology, Haifa 32000, Israel

²³Department of Physics and Astronomy, Tel Aviv University, Tel Aviv 69978, Israel

²⁴International Centre for Elementary Particle Physics and Department of Physics, University of Tokyo, Tokyo 113, and Kobe University, Kobe 657, Japan

²⁵Brunel University, Uxbridge, Middlesex UB8 3PH, UK

²⁶Particle Physics Department, Weizmann Institute of Science, Rehovot 76100, Israel

²⁷Universität Hamburg/DESY, II Institut für Experimental Physik, Notkestrasse 85, D-22607 Hamburg, Germany

²⁸University of Victoria, Department of Physics, P O Box 3055, Victoria BC V8W 3P6, Canada

²⁹University of British Columbia, Department of Physics, Vancouver BC V6T 1Z1, Canada

³⁰University of Alberta, Department of Physics, Edmonton AB T6G 2J1, Canada

³¹Duke University, Dept of Physics, Durham, NC 27708-0305, USA

³²Research Institute for Particle and Nuclear Physics, H-1525 Budapest, P O Box 49, Hungary

³³Institute of Nuclear Research, H-4001 Debrecen, P O Box 51, Hungary

³⁴Ludwigs-Maximilians-Universität München, Sektion Physik, Am Coulombwall 1, D-85748 Garching, Germany

^a and at TRIUMF, Vancouver, Canada V6T 2A3

^b and Royal Society University Research Fellow

^c and Institute of Nuclear Research, Debrecen, Hungary

^d and Department of Experimental Physics, Lajos Kossuth University, Debrecen, Hungary

1 Introduction

Currently there is no evidence that leptons are composite particles. If the known leptons are bound states of new elementary particles then excited states, called excited leptons and denoted here as ℓ^* , should exist.¹ Excited leptons have been searched for at the LEP e^+e^- collider at $\sqrt{s} = M_Z$ (\sqrt{s} is the centre-of-mass energy) [1, 2] and at the HERA ep collider [3]. The LEP searches and Z boson lineshape measurements rule out excited leptons with masses less than about $M_Z/2$, and for excited leptons with masses between $M_Z/2$ and M_Z they rule out ratios of coupling to compositeness scales (defined below) above about $(1 \text{ TeV})^{-1}$. The HERA searches for excited electrons reach to higher masses with less sensitivity, typically ruling out ratios of coupling to compositeness scales above about $(0.1 \text{ TeV})^{-1}$ up to masses around 250 GeV. Processes such as $e^+e^- \rightarrow \gamma\gamma$ are sensitive to excited particle states at still higher mass scales but have less sensitivity than direct searches if direct production is kinematically allowed [4, 5]. This paper presents results from a new search for e^* , μ^* , τ^* , ν_e^* , ν_μ^* , and ν_τ^* using the OPAL detector at $\sqrt{s} = 130 \text{ GeV}$ and 136 GeV .

Excited leptons can be pair produced in e^+e^- collisions via the process $e^+e^- \rightarrow \ell^*\bar{\ell}^*$, governed by the $\ell^*\ell^*V$ coupling, where V is a γ or Z vector boson. The excited leptons are assumed to have the same electroweak $SU(2)$ and $U(1)$ gauge couplings, g and g' , as the normal leptons, but are expected to be grouped in both left- and right-handed weak isodoublets. The existence of the right-handed doublets is required to protect the ordinary light leptons from radiatively acquiring a large anomalous magnetic moment via the $\ell^*\ell V$ interaction [6]. Here, to preserve consistency among the pair production, single production and decay models, we consider the full left- and right-handed doublets.

For excited lepton pair production, we have developed a Monte Carlo generator based on the formulae in Reference [6], including initial state radiation effects [7]. With $\sqrt{s} = 136 \text{ GeV}$, the pair production cross-sections for charged and neutral excited leptons are similar, and range from about 7 pb for a mass of 50 GeV to 3 pb for a mass of 65 GeV.

The production of single excited leptons and their decays are governed by the $\ell^*\ell V$ coupling. We use the effective Lagrangian [6]

$$\mathcal{L}\ell^* = \frac{1}{2\Lambda} \bar{\ell}^* \sigma^{\mu\nu} \left[gf \frac{\tau}{2} W_{\mu\nu} + g' f' \frac{Y}{2} B_\mu \right] \ell + \text{hermitian conjugate}, \quad (1)$$

which describes the generalized magnetic de-excitation of the ℓ^* states. The constants g and g' are the normal electroweak $SU(2)$ and $U(1)$ gauge couplings, $\sigma^{\mu\nu}$ is the covariant bilinear tensor, τ are the Pauli matrices, $W_{\mu\nu}$ are the electroweak isotriplet vector fields, B_μ is the electroweak singlet field, and Y is the weak hypercharge. The parameter Λ can be regarded as the ‘‘compositeness scale,’’ while f and f' are couplings associated with the different gauge groups. For excited lepton single production, we have developed a Monte Carlo generator based on the formulae in Reference [8], including initial state radiation effects [7].

In the Monte Carlo generation, we have required that the excited leptons decay via $\ell^* \rightarrow \ell V$, with an isotropic angular distribution in the ℓ^* rest frame. In general, the excited leptons will be produced in a polarised state, leading to a slightly non-isotropic decay distribution. It has been shown that the correct angular distributions for excited electron single production can be simply approximated [6, 8]. We have checked the effect of using the correct angular distribution

¹In this paper, ℓ refers to any charged lepton, ℓ^\pm , or neutral lepton, ν .

in our excited electron search, and found that it makes a negligible difference in the selection efficiency. Since the excited electron single production angular distribution is in any case not valid for any of the other modes, we choose the isotropic distribution for simplicity.

The three parameters f , f' and Λ in Equation (1) are arbitrary. To interpret the results of the searches for photonic decays of charged excited leptons and charged decays of neutral excited leptons, we adopt the coupling convention used in most previous experimental searches, $f = f'$. The model then reduces to one parameter, f/Λ . With this coupling assignment, the branching ratio for $\ell^{*\pm} \rightarrow \ell^\pm \gamma$ varies from essentially 100% for masses less than the W mass to about 45% for masses of 130 GeV, and the branching ratio for $\nu^* \rightarrow \ell^\pm W$ varies from about 80% for masses less than the W mass to about 70% for masses of 130 GeV. The W may be real or virtual depending on the ν^* mass.

With the $f = f'$ coupling assignment, photonic ν^* decays are forbidden. We arbitrarily consider the coupling assignment $f = -f'$ in our search for $\nu^* \rightarrow \nu \gamma$. With this coupling assignment, the photonic ν^* branching ratio varies from essentially 100% for masses less than the W mass to about 45% for masses of 130 GeV.

2 The OPAL Detector and Data Sample

A complete description of the OPAL detector can be found in Reference [9], and it is described only briefly here. The central detector consists of a system of tracking chambers that provides charged particle tracking over 96% of the full solid angle² inside a uniform 0.435 T magnetic field. It consists of a two layer silicon microstrip vertex detector, a high precision vertex drift chamber, a large volume jet chamber and a set of z chambers that measure the track coordinates along the beam direction. The ionization energy loss per unit path length in the jet chamber, dE/dx , is used for particle identification. A lead-glass electromagnetic calorimeter located outside the magnet coil covers the full azimuthal range with excellent hermeticity in the polar angle range of $|\cos \theta| < 0.82$ for the barrel region and $0.81 < |\cos \theta| < 0.984$ for the endcap region. The magnet return yoke is instrumented with streamer tubes with cathode strip readout for hadron calorimetry and consists of barrel and endcap sections along with pole tip detectors that together cover the region $|\cos \theta| < 0.99$. Muons are identified with the hadron calorimeter strips, and with four layers of muon chambers which cover the outside of the hadron calorimeter. The gamma catcher, forward detector and silicon tungsten electromagnetic calorimeters complete the geometrical acceptance down to 24 mrad. The forward detector and silicon tungsten calorimeters are used for the luminosity measurement.

The integrated luminosity used for this analysis is 2.5 pb^{-1} at $\sqrt{s} = 130 \text{ GeV}$ and 2.6 pb^{-1} at $\sqrt{s} = 136 \text{ GeV}$. Backgrounds from different Standard Model processes are estimated with several event generators, described in the analysis sections of the paper. All background and signal Monte Carlo samples are processed through the full OPAL detector simulation [10].

²The OPAL coordinate system is defined so that the z axis is in the direction of the electron beam and the x axis points towards the centre of the LEP ring; θ and ϕ are the polar and azimuthal angles, defined relative to the $+z$ - and $+x$ -axes, respectively.

3 Selection Criteria

This section of the paper first describes the general criteria used to select events consistent with excited lepton production, and then describes the lepton and photon identification and isolation requirements used in the analyses. In Sections 3.1, 3.2, and 3.3, we describe the search for the photonic decays of excited charged leptons in $\ell^+\ell^-\gamma\gamma$, $\ell^+\ell^-\gamma$, and $e\gamma$ topologies, respectively. Next, in Section 3.4 we describe the search for charged decays of excited neutral leptons in $\ell^+\ell^-WW$ and $\nu\ell^\pm W$ topologies. Finally, in Section 3.5 we describe the search for the photonic decays of excited neutral leptons in events with purely photonic final states.

In order to be considered in the analysis, tracks in the central detector and clusters of energy in the electromagnetic calorimeter must satisfy the normal quality criteria employed in the analysis of lepton pairs [11]. In addition, a “good” track must satisfy $|\cos\theta| < 0.95$ and have an associated electromagnetic calorimeter cluster.

A preselection is performed to remove obvious background events. Cosmic rays and multihadronic events are rejected using standard algorithms as described in the analysis of muon pairs [11]. Beam-gas and beam-wall collision events are rejected by requiring that the ratio of the number of good charged tracks to the total number of charged tracks reconstructed in the central detector be greater than 0.2.

Tracks with $p > 1.5$ GeV (where p is the track momentum) are considered as potential lepton candidates, and the following, non-exclusive, identification requirements are made:

muon: a track is identified as a muon if it satisfies either of the following two criteria:

1. The track is identified as a muon according to the criteria employed in the analysis of muon pairs [11]. That is, it has associated activity in the muon chambers or hadron calorimeter strips or it has a high momentum but is associated with only a small energy deposition in the electromagnetic calorimeter.
2. The track is identified as a muon according to the criteria employed in the analysis of inclusive muons in multihadronic events [12]. This second criterion is desirable to recover some extra efficiency for low energy recoil muons in the single production search.

The muon is required to be “isolated” by demanding that the sum of the momenta of all other tracks within a cone of 20° half-opening-angle centred on the track is less than 1 GeV, and the sum of the energies of all additional clusters within the same cone is also less than 1 GeV. The energy, E_μ , and the direction of the muon are computed using the track observed in the central detector.

electron: a track which is not identified as a muon is identified as an electron if it satisfies any of the following three criteria:

1. $0.8 < E/p < 1.3$, where p is the momentum of the track and E is the energy of the associated electromagnetic cluster.
2. $0.5 < E/p < 2.0$ and dE/dx is consistent with that expected from an electron.
3. The output of the electron identification neural network described in Reference [13] is greater than 0.8. This final criterion is desirable to recover some extra efficiency for low energy recoil electrons in the single production search.

The electron is required to be isolated using the same criteria as for muons. The energy, E_e , of the electron is computed using the electromagnetic calorimeter cluster energy, and its direction is computed using the track observed in the central detector.

tau: a track is identified as originating from a tau decay if it satisfies either of the following two conditions:

1. It is identified as an electron or muon according to the above requirements (i.e. electrons and muons are also used as tau candidates).
2. There are at most two additional tracks in a cone with a half-angle of 35° (i.e. up to 3 tracks in total).

A tau “jet” is constructed by adding the momenta of all tracks and clusters inside the 35° half-angle cone. The tau energies, E_τ , are calculated by assuming that the tau direction is the same as the jet direction, using only the energy of the photon(s) (the photon identification requirements are described next) and the angles between the photon(s) and the jets. This calculation implicitly assumes that the two taus and the observed photon(s) make up the entire final state.

A separate search is performed to identify photons:

photon: A photon candidate must satisfy either of the following two criteria:

1. An electromagnetic cluster with no associated good charged tracks.
2. A photon conversion identified with the algorithm employed in the analysis of muon pairs [11]. The tracks and clusters associated with the conversion are combined to form a single 4-vector representing the photon.

Photons are required to be isolated using the same criteria as for muons and electrons. The photon is also required to satisfy $|\cos\theta| < 0.95$ and to have an energy greater than 1 GeV.

3.1 $\ell^{*\pm}$ Pair Production: $\ell^+\ell^-\gamma\gamma$ Topologies

Candidate $\ell^+\ell^-\gamma\gamma$ events are required to satisfy the following criteria:

1. There must be at least two identified leptons of the same type and at least two photons. The two most energetic leptons and two most energetic photons are used for further analysis.
2. With two leptons and two photons, there are two possible ways of forming two lepton-photon mass combinations for each event. At least one of the two ways must have a difference between the mass combinations less than 10 GeV and an average mass greater than 30 GeV.

The two lepton-photon invariant masses are plotted against each other after cut 1 in Figure 1. After both cuts, no candidates are observed in the data for any channel.

In the $ee\gamma\gamma$ analysis, after cut 1 a total of 2.8 background events is expected with 1 event observed in the data, and after cut 2 a total of 0.3 background events is expected. The dominant background is from radiative Bhabha scattering, evaluated with the radiative e^+e^- event generator BHWIDE [14]. In the $\mu\mu\gamma\gamma$ analysis, after cut 1 a total of 1.5 background events is expected with 2 events observed in the data, and after cut 2 a total of 0.2 background events is expected. The dominant background is from radiative muon pair production, evaluated with the radiative $\ell^+\ell^-$ event generator KORALZ [15]. In the $\tau\tau\gamma\gamma$ analysis, after cut 1 a total of 7.6 background events is expected with 7 events observed in the data, and after cut 2 a total of 0.7 background events is expected. The background has contributions from radiative Bhabha scattering (evaluated with BHWIDE), from radiative muon pair production (evaluated with KORALZ), from radiative tau pair production (evaluated with KORALZ), and from multihadronic events (evaluated with the JETSET 7.4 parton shower event generator [16]).

The efficiency for observing the pair production of excited leptons was evaluated at four selected masses above 50 GeV at $\sqrt{s}=130$ GeV and $\sqrt{s}=136$ GeV and was found to be independent of the centre-of-mass energy and of the excited lepton mass in the kinematic region of interest. The efficiency was found to be 0.579 ± 0.006 for e^*e^* , 0.641 ± 0.006 for $\mu^*\mu^*$ and 0.431 ± 0.006 for $\tau^*\tau^*$, where the errors are from Monte Carlo statistics.

3.2 $\ell^{*\pm}$ Single Production: $\ell^+\ell^-\gamma$ Topologies

Candidate $\ell^+\ell^-\gamma$ events are required to satisfy the following criteria:

1. There must be at least two identified leptons of the same type, at least one of which must have energy $E_\ell > 0.3E_{\text{beam}}$, and exactly one photon with energy $E_\gamma > 0.3E_{\text{beam}}$, where E_{beam} is the beam energy. The two most energetic leptons and the photon are used for further analysis.
2. The two leptons and the photon must account for more than 80% of the centre-of-mass energy.
3. (a) For the e^* search, radiative Bhabha scattering is suppressed by requiring that the photon and at least one electron satisfy $|\cos\theta| < 0.7$.
(b) For the τ^* search, radiative Bhabha scattering and di-muon events are suppressed by requiring that the energy sum of the 2 jets corresponding to the tau candidates and the one photon satisfy $E_{\text{jet},1} + E_{\text{jet},2} + E_\gamma < 1.8E_{\text{beam}}$.
4. The process $e^+e^- \rightarrow Z\gamma \rightarrow \ell^+\ell^-\gamma$ is suppressed by vetoing events with $M_{\ell\ell} > 80$ GeV, where $M_{\ell\ell}$ is the invariant mass of the pair of leptons.

After all cuts, two events are observed in the $ee\gamma$ analysis, no events in the $\mu\mu\gamma$ analysis, and two events in the $\tau\tau\gamma$ analysis. With two leptons and one photon, there are two possible lepton-photon mass combinations for each event. The $\ell^\pm\gamma$ invariant mass distributions for both combinations are plotted in Figure 2(a), (c) and (d) for e^* , μ^* and τ^* , respectively.

In the $ee\gamma$ analysis, a total of 2.3 background events is expected. The dominant background is from radiative Bhabha scattering, evaluated with BHWIDE. In the $\mu\mu\gamma$ analysis, a total of 1.7 background events is expected. The dominant background is from radiative muon pair events,

evaluated with KORALZ. In the $\tau\tau\gamma$ analysis, a total of 2.4 background events is expected. The background has contributions from radiative Bhabha scattering (evaluated with BHWIDE), muon pair (evaluated with KORALZ) and tau pair events (evaluated with KORALZ). The number of observed events is compatible with the expectation from Standard Model sources, and we conclude that there is no evidence for excited lepton production in these topologies.

When computing limits for an excited lepton with mass M_* , all events with at least one lepton-photon mass combination, $M_{\ell\gamma}$, satisfying $|M_{\ell\gamma} - M_*| < \Delta$ were considered signal candidates. The mass half-window, Δ , is 4 GeV, 8 GeV and 8 GeV for e^* , μ^* and τ^* , respectively (the values chosen for Δ are about 2σ of the mass resolution estimated with Monte Carlo). The efficiency for observing the single production of excited leptons was evaluated after the mass window requirement for four selected masses at $\sqrt{s} = 130$ GeV and $\sqrt{s} = 136$ GeV, and the efficiency at an arbitrary mass is estimated from the linear interpolation between two of these points. The efficiency varies from 34% at a mass of 70 GeV to 75% at a mass of 130 GeV for μ^* and from 24% to 47% for τ^* . The efficiency for the $ee\gamma$ analysis is evaluated after combining it with the analysis presented in Section 3.3.

3.3 e^* Single Production: $e\gamma$ Topology

A significant fraction of singly produced e^* events would have the recoil electron at a small polar angle outside our detector acceptance, making the search for the $e\gamma$ final state also desirable. For the $e\gamma$ final state analysis, the energy and direction of the missing electron are inferred using conservation of momentum from the observed electron and photon by assuming an $ee\gamma$ topology.

Candidate $e\gamma$ events are required to satisfy the following criteria:

1. There must be exactly one identified electron with energy $E_e > 0.3E_{\text{beam}}$ and exactly one photon with energy $E_\gamma > 0.3E_{\text{beam}}$.
2. The observed e^\pm , the inferred missing e^\mp , and the photon must account for more than 80% of the centre-of-mass energy.
3. Bhabha scattering is suppressed by requiring the photon to satisfy $|\cos\theta_\gamma| < 0.7$.
4. The missing particle is required to be consistent with the production hypothesis by demanding $p_T^{\text{miss}} < 0.4E_{\text{beam}}$ and $Q_e \times \cos\theta_{\text{miss}} > 0.8$, where p_T^{miss} is transverse component of the momentum of the missing electron, θ_{miss} is the polar angle of the missing electron and Q_e is the charge of the observed electron.

After all cuts, 17 events are observed in the $e\gamma$ analysis. The $e\gamma$ invariant mass distribution for this topology is plotted in Figure 2(b).

A total of 21.2 background events is expected. The dominant background for this topology is from t -channel radiative Bhabha scattering, evaluated with the radiative e^+e^- event generator TEEGG [17]. The number of observed events is compatible with the expectation from Standard Model sources and there is no peak in the electron-photon mass distribution. We conclude that there is no evidence for excited electron production in this topology.

When computing limits for an excited electron with mass M_* , all events with an electron-photon invariant mass, $M_{e\gamma}$, satisfying $|M_{e\gamma} - M_*| < 4$ GeV were considered signal candidates (about 2σ of the mass resolution estimated with Monte Carlo). The efficiency for the observation of the single production of e^* is evaluated after the mass window requirement for the combination of the $ee\gamma$ and $e\gamma$ analyses using the interpolation method described in Section 3.2, and varies from 44% at a mass of 70 GeV to 57% at a mass of 130 GeV.

3.4 ν^* Production: $\ell^+\ell^-WW$ and $\nu\ell^\pm W$ Topologies

The search for charged decays of pair produced excited neutrinos uses the search for the production of unstable heavy neutral leptons described in [18]. The topology $e^+e^- \rightarrow L^0\bar{L}^0 \rightarrow \ell^+\ell^-WW$ is almost identical to excited neutrino pair production with charged decays. The heavy lepton analysis observed no candidate event with an expected background of 0.70 events from all Standard Model sources. The efficiency for the observation of the pair production of ν^* which undergo charged decays is about 55% for $\nu_e^*\bar{\nu}_e^* \rightarrow e^+e^-WW$, 60% for $\nu_\mu^*\bar{\nu}_\mu^* \rightarrow \mu^+\mu^-WW$ and 30% for $\nu_\tau^*\bar{\nu}_\tau^* \rightarrow \tau^+\tau^-WW$ (the W bosons are always virtual in the mass region accessible to this analysis).

The search for charged decays of singly produced excited neutrinos looks only for leptonic decays of the W, which may be real or virtual depending on the mass of the ν^* . The search then looks for $e^+e^- \rightarrow \nu_\ell\nu_\ell^* \rightarrow \nu_\ell\ell^\pm W \rightarrow \nu_\ell\ell^\pm\nu_{\ell'}\ell'^\mp$, where ℓ^\pm corresponds to the excited neutrino flavour, and ℓ'^\mp may or may not be of the same type. The topology is a pair of leptons which are not coplanar with the beam direction.

Candidate ν_ℓ^* events are required to satisfy the following criteria:

1. There must be two identified leptons, at least one of type ℓ^\pm . At least one of the leptons must have an energy greater than $0.2E_{\text{beam}}$.
2. There must be no other good track in the event.
3. Excluding the clusters associated with the two leptons, the sum of other barrel and endcap electromagnetic calorimeter cluster energies must be less than 2 GeV.
4. Two-photon and multihadronic events are vetoed by requiring that there is no significant energy in either side of the forward detector (less than 2 GeV), silicon tungsten (less than 5 GeV), or gamma catcher (less than 5 GeV) electromagnetic calorimeters.
5. Events with energy missing along the beam axis are removed by requiring $|\cos\theta_{\text{miss}}| < 0.9$, where $\cos\theta_{\text{miss}}$ is the cosine of the polar angle of the missing momentum.
6. Events are required to be acoplanar by requiring $\phi_{\ell\ell}^{\text{ACOP}} > 20^\circ$ ($\phi_{\ell\ell}^{\text{ACOP}}$ is the complement of the angle between the two leptons in the xy plane).

No event was observed after all the cuts. A total of 0.15 background events is expected for ν_e^* , 0.15 background events for ν_μ^* and 0.33 background events for ν_τ^* . The dominant background is from four fermion processes, evaluated using the event generator described in Reference [19].

The efficiency is about 20% for ν_e^* and ν_μ^* , and about 15% for ν_τ^* . There is a small dependence on the ν^* mass, which is taken into account in the results. The efficiency is small because we use only leptonic W decays.

3.5 ν^* Production: $\nu\bar{\nu}\gamma\gamma$ and $\nu\bar{\nu}\gamma$ Topologies

For the pair production $\nu^*\bar{\nu}^* \rightarrow \nu\bar{\nu}\gamma\gamma$ analysis, the acoplanar di-photon analysis (“Topology B”) in the OPAL analysis of photonic final states [4] is used. That analysis observed four events with an expected background of 0.7 events from $e^+e^- \rightarrow Z\gamma\gamma \rightarrow \nu\bar{\nu}\gamma\gamma$, evaluated using the event generator NNGG03 [20]. We make an additional requirement that both observed photons are kinematically consistent with the decay of a ν^* of a given mass. Specifically, each photon must satisfy $0.9 E_\gamma^{\min} < E_\gamma < 1.1 E_\gamma^{\max}$, where E_γ is the photon energy and E_γ^{\min} (E_γ^{\max}) is the minimum (maximum) allowed photon energy given a specific ν^* mass with the known centre-of-mass energy. Based on this criterion, the four selected events in Reference [4] are found to be kinematically consistent with $\nu^*\bar{\nu}^*$ production for $M_{\nu^*} < 20$ GeV. No event is kinematically consistent with a ν^* mass exceeding 40 GeV. The expected background from $\nu\bar{\nu}\gamma\gamma$ from NNGG03 is 0.7 for a ν^* mass of 20 GeV, 0.5 for a ν^* mass of 40 GeV and 0.1 for a ν^* mass of 60 GeV. As noted in Reference [4], the observed number of events consistent with a ν^* mass of 20 GeV exceeds the expectation, but the kinematic characteristics are consistent with the photon pair recoiling against a Z as expected from the $e^+e^- \rightarrow Z\gamma\gamma \rightarrow \nu\bar{\nu}\gamma\gamma$ background process. The efficiency for observing the pair production of excited neutrinos with photonic decays was evaluated at four selected masses above 50 GeV at $\sqrt{s}=130$ GeV and $\sqrt{s}=136$ GeV and was found to be independent of the centre-of-mass energy and of the excited neutrino mass. The efficiency was found to be 0.362 ± 0.006 for each excited neutrino flavour.

For the single production $\nu^*\nu \rightarrow \nu\bar{\nu}\gamma$ analysis, the single photon analysis (“Topology A”) in Reference [4] is used. That analysis found 19 events with an expected background of 19.2 events from $e^+e^- \rightarrow \nu\bar{\nu}\gamma$ evaluated with NNGG03. We make an additional requirement that the event be inconsistent with the process $e^+e^- \rightarrow Z\gamma \rightarrow \nu\bar{\nu}\gamma$. Specifically, events with $M_{\text{miss}} > 80$ GeV are removed from the sample, where M_{miss} is the missing mass in the event. With this additional requirement, no event survives from the single photon analysis in Reference [4], which is consistent with the expectation from NNGG03 of 0.1 events. The efficiency varies from about 25% at a mass of 70 GeV to about 55% at a mass of 130 GeV. The t -channel production diagram causes the efficiency for ν_e^* to be slightly different from ν_μ^* and ν_τ^* , and the efficiencies are evaluated separately.

4 Results

The systematic errors in the total number of expected signal events are estimated from: the statistical error on the Monte Carlo estimate of the detection efficiency; the systematic error on the integrated luminosity (0.9%); uncertainties in the modelling of the particle identification cuts (2.5% if one identified lepton is required, 5% if two are required); uncertainties in the modelling of the photon conversion finder (1% per photon in the event). The errors are considered to be independent and are added in quadrature for the total systematic error. The systematic error is incorporated into the limits using the method described in Reference [21].

In the Monte Carlo generation of simulated signal and cross-section calculations, integrated luminosities of 2.5 pb^{-1} at a beam energy of 65.0 GeV and 2.6 pb^{-1} at a beam energy of 68.0 GeV were assumed. The actual beam energies were estimated to be 65.13 ± 0.03 GeV and 68.12 ± 0.03 [22], making the limits slightly conservative. No background subtractions are performed when calculating limits in any channel.

The production cross-sections from Reference [6] (corrected for the effects of initial state radiation), branching ratios from References [6] and [23] and measured efficiencies are used to calculate the number of events expected for an excited lepton of a given mass. Poisson statistics with the number of observed events are used to set limits on the maximum number of events in each analysis.

For the pair production searches, limits on the excited lepton masses are inferred. The 95% confidence level lower mass limits are listed in Table 1, along with the coupling assumptions which are used for the branching ratio calculation for each topology.

For the single production searches, limits on the ratio of the coupling to the compositeness scale, f/Λ , are inferred. Limits on f/Λ for charged excited leptons with $f = f'$ are plotted in Figure 3(a), limits on f/Λ for neutral excited leptons with $f = f'$ from the W decay mode search are plotted in Figure 3(b), and limits on f/Λ for neutral excited leptons with $f = -f'$ from the γ decay mode search are plotted in Figure 3(c). In Figure 3(a), results from $\sqrt{s} = M_Z$ are used for excited lepton masses less than about 90 GeV. These LEP1 results used an analysis similar to Reference [1], updated to an integrated luminosity of 6.35 pb^{-1} ; the e^* and μ^* analyses are identical to those in Reference [1], while the τ^* analysis included an estimate of the tau momentum (and therefore the τ - γ mass) similar to this paper.

Flavour	Decays	Coupling	Mass Limit
e^*	Photonic	$f = f'$	66.5 GeV
μ^*	Photonic	$f = f'$	66.8 GeV
τ^*	Photonic	$f = f'$	65.3 GeV
ν_e^*	Charged	$f = f'$	66.2 GeV
ν_μ^*	Charged	$f = f'$	66.2 GeV
ν_τ^*	Charged	$f = f'$	64.7 GeV
ν_e^*	Photonic	$f = -f'$	65.0 GeV
ν_μ^*	Photonic	$f = -f'$	65.0 GeV
ν_τ^*	Photonic	$f = -f'$	65.0 GeV

Table 1: 95% confidence level lower mass limits for the different excited leptons from the pair creation searches. The coupling assumption is necessary for the branching ratio calculation.

5 Conclusion

We have analysed a data sample with an integrated luminosity of 2.5 pb^{-1} at 130 GeV and 2.6 pb^{-1} at 136 GeV, collected with the OPAL detector at LEP, to search for the production of excited leptons. No evidence for excited leptons was found, and limits on masses and couplings are established within the framework of the model in Reference [6]. From the search for pair production, lower mass limits are established for charged excited leptons which undergo photonic decays and for neutral excited leptons which undergo either photonic or charged decays. From the search for single production, upper limits on the ratio of the coupling to the compositeness scale are established. This analysis has similar sensitivity to other results reported from the LEP 1995 run at $\sqrt{s} = 130 - 140 \text{ GeV}$ [24] but includes additional results for excited muon and tau neutrino decays.

6 Acknowledgements

We particularly wish to thank the SL Division for the efficient operation of the LEP accelerator and for their continuing close cooperation with our experimental group. In addition to the support staff at our own institutions we are pleased to acknowledge the
Department of Energy, USA,
National Science Foundation, USA,
Particle Physics and Astronomy Research Council, UK,
Natural Sciences and Engineering Research Council, Canada,
Israel Ministry of Science,
Israel Science Foundation, administered by the Israel Academy of Science and Humanities,
Minerva Gesellschaft,
Japanese Ministry of Education, Science and Culture (the Monbusho) and a grant under the Monbusho International Science Research Program,
German Israeli Bi-national Science Foundation (GIF),
Direction des Sciences de la Matière du Commissariat à l’Energie Atomique, France,
Bundesministerium für Bildung, Wissenschaft, Forschung und Technologie, Germany,
National Research Council of Canada,
Hungarian Foundation for Scientific Research, OTKA T-016660, and OTKA F-015089.

References

- [1] OPAL Collaboration, M. Z. Akrawy *et al.*, Phys. Lett. B 257 (1990) 531.
- [2] ALEPH Collaboration, D. Decamp *et al.*, Phys. Lett. B 250 (1990) 172;
DELPHI Collaboration, P. Abreu *et al.*, Z. Phys. C53 (1992) 41;
L3 Collaboration, M. Acciarri *et al.*, Phys. Lett. B 353 (1995) 136.
- [3] H1 Collaboration, I. Abt *et al.*, Nucl. Phys. B 396 (1993) 3;
ZEUS Collaboration, M. Derrick *et al.*, Z. Phys. C65 (1994) 627.
- [4] OPAL Collaboration, G. Alexander *et al.*, “Measurements with Photonic Events in e^+e^- Collisions at Centre-of-Mass Energies of 130-140 GeV,” CERN-PPE/96-039 (1996), to be published in Phys. Lett. B.
- [5] L3 Collaboration, M. Acciarri *et al.*, Phys. Lett. B 353 (1995) 136;
L3 Collaboration, M. Acciarri *et al.*, “Search for Excited Leptons in e^+e^- Annihilation at $\sqrt{s} = 130-140$ GeV,” CERN-PPE/96-48 (1996), submitted to Phys. Lett. B;
ALEPH Collaboration, D. Buskulic *et al.*, “A study of single and multi-photon production in e^+e^- collisions at centre-of-mass energies of 130 and 136 GeV,” CERN-PPE/96-53 (1996), submitted to Phys. Lett. B.
- [6] F. Boudjema, A. Djouadi, J. L. Kneur, Z. Phys. C57 (1993) 425.
- [7] The initial state radiation is implemented according to the formulae in F. A. Berends, R. Pittau and R. Kleiss, Nucl. Phys. B 426 (1994) 344.

- [8] K. Hagiwara, S. Komamiya, and D. Zeppenfeld, *Z. Phys.* C29 (1985) 115.
- [9] OPAL Collaboration, K. Ahmet *et al.*, *Nucl. Instr. Meth. A* 305 (1991) 275;
P. P. Allport *et al.*, *Nucl. Instr. Meth. A* 324 (1993) 34;
P. P. Allport *et al.*, *Nucl. Instr. Meth. A* 346 (1994) 476;
B. E. Anderson *et al.*, *IEEE Trans. Nucl. Sci.* 41 (1994) 845.
- [10] J. Allison *et al.*, *Nucl. Instr. Meth. A* 317 (1992) 47.
- [11] OPAL Collaboration, G. Alexander *et al.*, *Z. Phys.* C52 (1991) 175.
- [12] OPAL Collaboration, P. Acton *et al.*, *Z. Phys.* C58 (1993) 523.
- [13] OPAL Collaboration, R. Akers *et al.*, *Phys. Lett. B* 327 (1994) 411.
- [14] S. Jadach, W. Placzek and B. F. L. Ward, University of Tennessee preprint, UTHEP 95-1001 (unpublished).
- [15] S. Jadach, B. F. L. Ward and Z. Wąs, *Comp. Phys. Comm.* 79 (1994) 503.
- [16] T. Sjöstrand, *Comp. Phys. Comm.* 82 (1994) 74.
- [17] D. Karlen, *Nucl. Phys. B* 289 (1987) 23.
- [18] OPAL Collaboration, G. Alexander *et al.*, “Search for Unstable Neutral and Charged Heavy Leptons in e^+e^- Collisions at $\sqrt{s} = 130$ and 136 GeV,” CERN-PPE/96-xxx, (1996), to be submitted to *Phys. Lett. B*.
- [19] The calculation of the cross-section is based on the method described in the preprint by H. Murayama, I. Watanabe and K. Hagiwara, KEK Report 91-11 (1991). The initial state radiation is implemented as in [7].
- [20] F. A. Berends *et al.*, *Nucl. Phys. B* 301 (1988) 583;
R. Miquel, C. Mana and M. Martinez, *Z. Phys.* C48 (1990) 309.
- [21] R. D. Cousins and V. L. Highland, *Nucl. Instr. Meth. A* 320 (1992) 331.
- [22] OPAL Collaboration, G. Alexander *et al.*, “Measurement of cross-sections and asymmetries in e^+e^- collisions at 130-140 GeV centre-of-mass energy,” CERN-PPE/96-025, (1996), to be published in *Phys. Lett. B*.
- [23] F. Boudjema and A. Djouadi, *Phys. Lett. B* 240 (1990) 485.
- [24] L3 Collaboration, M. Acciarri *et al.*, *Phys. Lett. B* 370 (1996) 211;
DELPHI Collaboration, P. Abreu *et al.*, “Study of radiative leptonic events with hard photons and search for excited charged leptons at $\sqrt{s} = 130$ - 136 GeV,” CERN-PPE/96-60, (1996), submitted to *Phys. Lett. B*.

OPAL

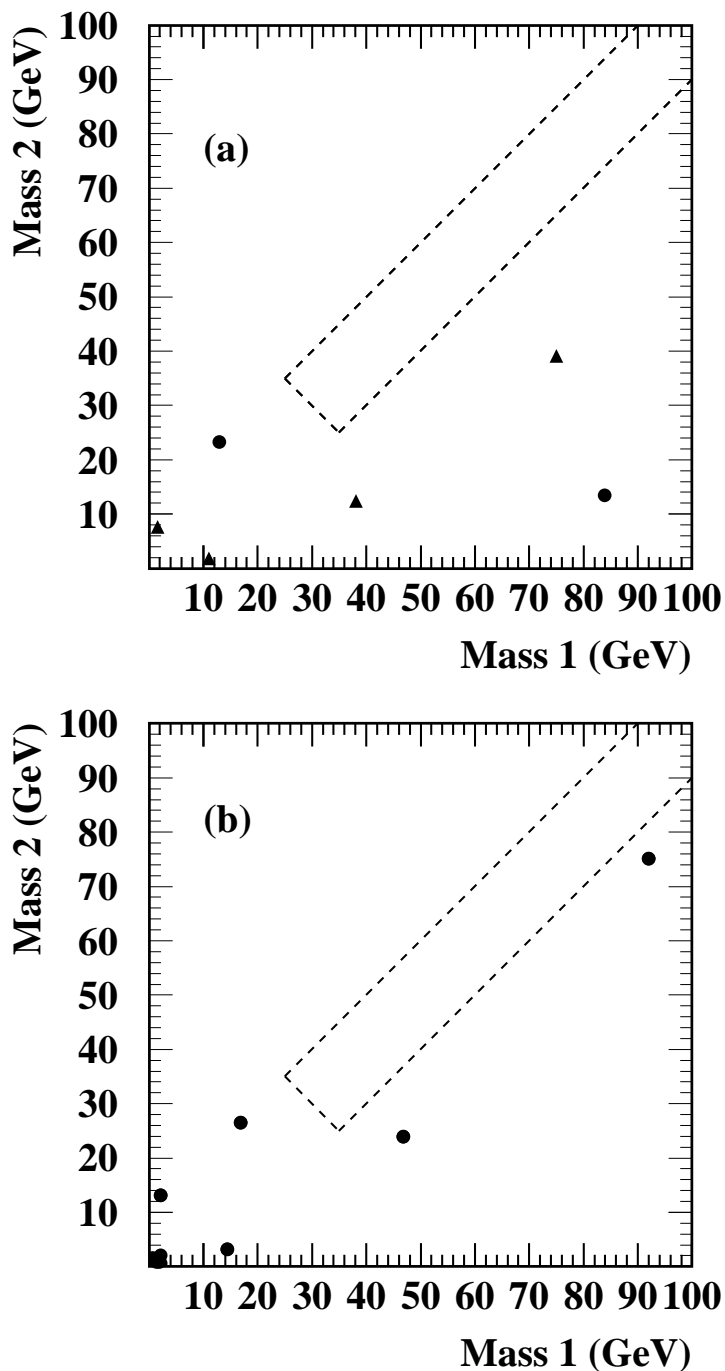


Figure 1: $\ell^{*\pm}$ pair production: both lepton-photon invariant mass combinations for each event surviving cut 1 in Section 3.1. (a) is for e^* (circles) and μ^* (triangles) and (b) is for τ^* . Mass 1 corresponds to masses computed with the higher energy lepton, and mass 2 to masses computed with the lower energy lepton. The dashed line corresponds to the allowed mass region, cut 2 in Section 3.1.

OPAL

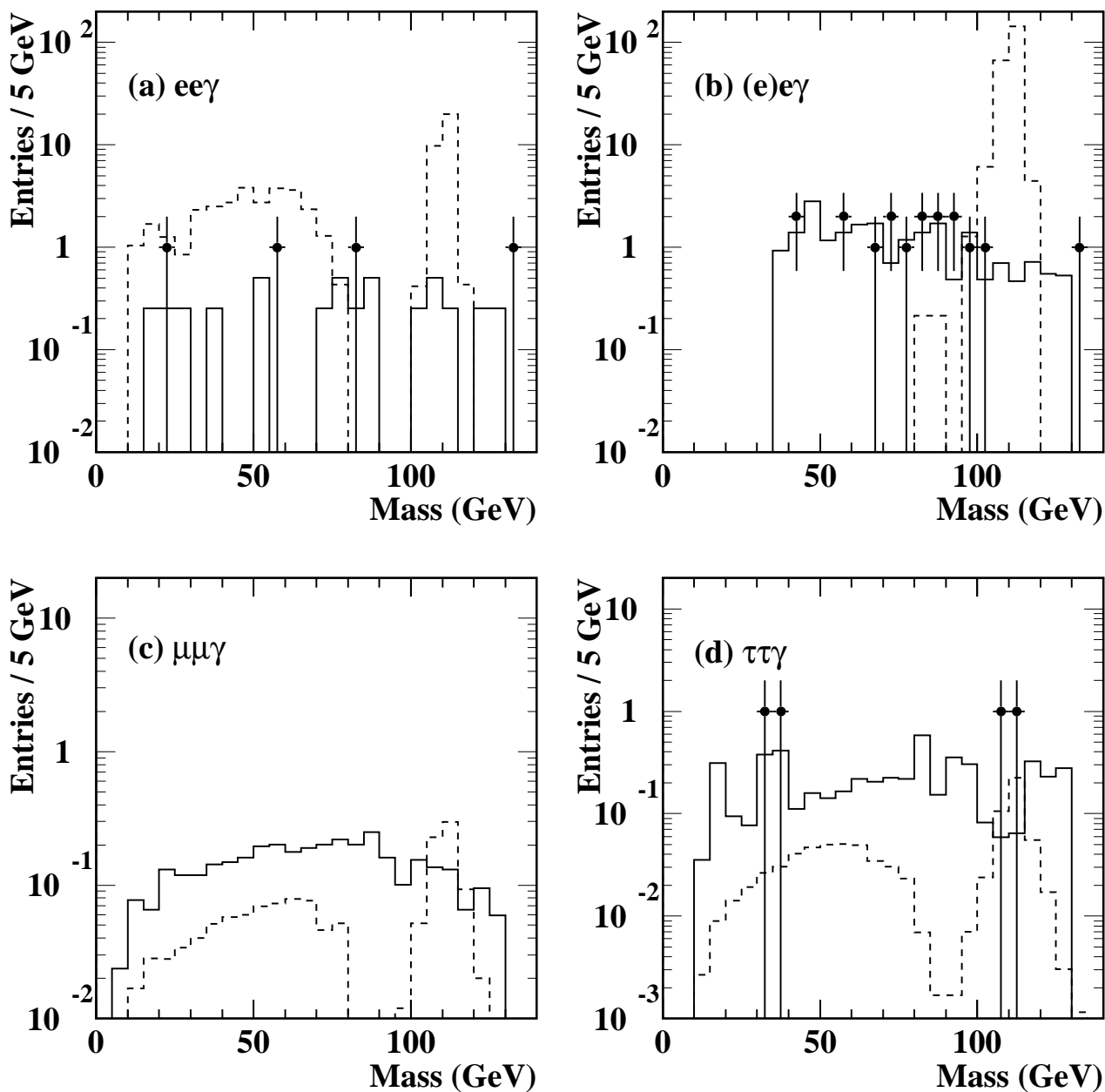


Figure 2: $\ell^{*\pm}$ single production: lepton-photon invariant mass distribution after all cuts. (a) is for e^* with two visible final state electrons, (b) is for e^* with one visible final state electron, (c) is for μ^* (no observed candidates) and (d) is for τ^* . The dashed lines are the signal Monte Carlo with a 110 GeV $\ell^{*\pm}$ mass and $f/\Lambda = (200 \text{ GeV})^{-1}$, the solid lines are the sum of all of the Standard Model background Monte Carlos and the filled circles are the full data set. In (a), (c) and (d), both mass combinations are plotted for each event.

OPAL

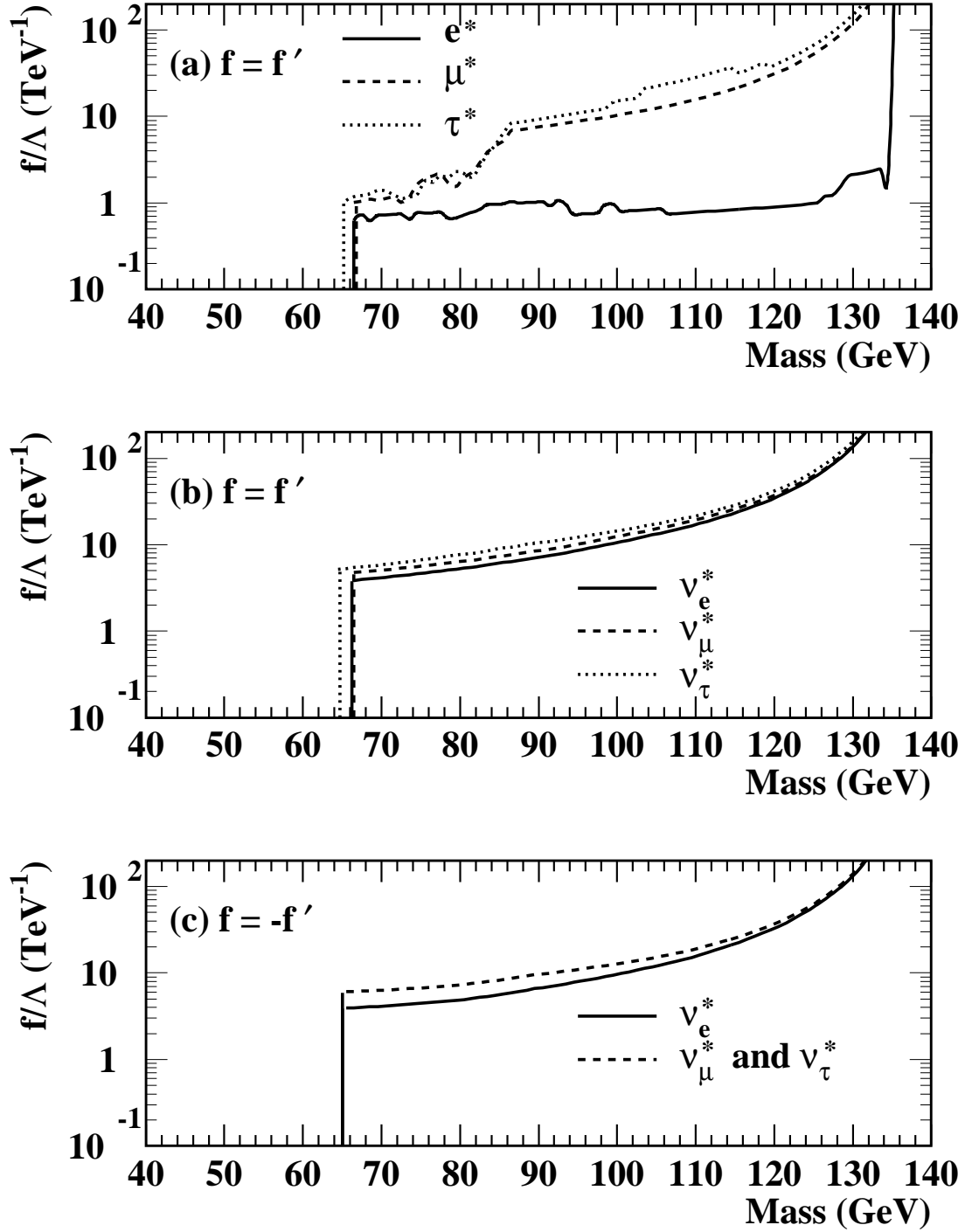


Figure 3: 95% confidence level upper limits on the ratio of the the coupling to the compositeness scale, f/Λ , as a function of the excited lepton mass. (a) shows the limits on e^* , μ^* and τ^* with $f = f'$, (b) shows the limits on ν_e^* , ν_μ^* and ν_τ^* with $f = f'$, and (c) shows the limits on ν_e^* , ν_μ^* and ν_τ^* with $f = -f'$. The regions above and to the left of the curves are excluded by the single and pair production searches, respectively.